hydrology

MDPI

Article

Quantifying Streambed Dispersion in an Alluvial Fan Facing the Northern Italian Apennines: Implications for Groundwater Management of Vulnerable Aquifers

Federico Cervi [1,2,*] and Alberto Tazioli [3]

[1] Independent Researcher, 42122 Reggio Emilia, Italy
[2] Department of Civil, Chemical, Environmental and Materials Engineering, University of Bologna, 40136 Bologna, Italy
[3] Dipartimento di Scienze e Ingegneria della Materia, dell'Ambiente ed Urbanistica, Università Politecnica delle Marche, 60131 Ancona, Italy; a.tazioli@staff.univpm.it
* Correspondence: fd.cervi@gmail.com

Abstract: Groundwater management of alluvial aquifers facing the northern Italian Apennines is an important issue that is becoming more complicated due to ongoing climate changes and increased water demands. The large groundwater withdrawals, coupled with an overall worsening of the water quality, require detailed knowledge of the recharge mechanisms of these aquifers that can be useful for further adaptation measures. We have focused our attention on a selected alluvial fan in which 49 slug injections of hyperconcentrated solutions of NaCl allowed river discharges to be estimated in seven different hydraulic sections. Consequently, losses from the streambed were assessed for the six river reaches along with the corresponding uncertainties in the estimates. The study confirms the suitability of such tests for identifying sectors in which streambed losses are promoted and for quantifying the total recharge conveyed to underlying aquifers. In addition, it has been demonstrated that the total streambed losses can be further linked to river discharges in any gauge upstream of the alluvial fan thanks to linear regression. Once obtained, the latter makes monitoring groundwater recharge by stream losses in real time possible if a permanent measurement device (such as the common telemetry used for river discharge monitoring) is available.

Keywords: dilution gauging; tracing test; groundwater; aquifer; alluvial fan; northern Apennines; Italy

Citation: Cervi, F.; Tazioli, A. Quantifying Streambed Dispersion in an Alluvial Fan Facing the Northern Italian Apennines: Implications for Groundwater Management of Vulnerable Aquifers. *Hydrology* **2021**, *8*, 118. https://doi.org/10.3390/hydrology8030118

Academic Editors: Brindha Karthikeyan, David Brauer, Nathan Howell and Ryan Bailey

Received: 19 June 2021
Accepted: 2 August 2021
Published: 7 August 2021

1. Introduction

Alluvial fans facing the northern Italian Apennines are pivotal for the water management of the most densely populated areas in the Emilia-Romagna region. Due to the simultaneous presence of a limited number of high-yield springs in the mountainous areas and rivers in which hydrological behavior closely follows the precipitation patterns (with marked low flow at the end of the summer period), the aquifers from the alluvial fans host the most important groundwater resources to ensure water supply. Here, wells provide hundreds of millions of m^3/y of water for both human consumption and agricultural/industrial purposes (about 740 Mm^3/y in the period 2002–2006 [1]). The northern Italian Apennines chain bedrock is made up of impermeable clayey materials (no subsurface flow from the adjacent mountains can take place) and groundwater recharge of the aquifers hosted in these alluvial fans is focused in reduced areas at the foothills of the mountain chain (i.e., apices of their alluvial fans), where coarser sediments such as sands and gravels are widespread [2,3]. Being characterized by the highest permeabilities, these sediments allow for both zenithal infiltration of meteoric water and streambed dispersion [3–5]. Thus, from the hydrogeological point of view, apices of the alluvial fans represent sensitive areas; the qualitative status and quantitative balance of these areas can be altered by both anthropogenic activities and variations in rainfall/river discharges. Indeed, the ongoing

monitoring of qualitative and quantitative status of groundwater from the apical part of these alluvial aquifers has indicated an overall worsening of some indicators such as deepening of groundwater levels (that in several cases has induced a drop in the order of several meters; see, for instance, [6]) and increase of pollutants (for instance, nitrates linked to zootechnical activities; [3,7]). In detail, the qualitative aspects of the groundwater hosted in the alluvial fans facing the northern Italian Apennines have been extensively studied in the literature [3,8–11] and have demonstrated that the origin of the impacts here is limited to point source or diffusive pollution phenomena conveyed to the groundwater directly through the streambed or by anthropic activities on the ground. Conversely, the worsening of the quantitative status could mainly be related to three factors.

First, an overexploitation of these aquifers with respect to the actual recharge rate by streambed dispersion and/or rainfall percolation from the topsoil may have led to an overall decrease in the groundwater levels that has been already highlighted [12,13]. Second, [14,15] reported that, starting from the 1970s, significant land use changes in the mountainous sector of catchments (such as dam constructions, river diversion developments, torrent control works, and extensive bed material mining) have occurred. The latter caused important sediment budget changes, which have in turn led to significant alterations of the channel morphologies in the apical part of the alluvial fans. Here, reduction and deepening (even of tens of meters) of the streambeds have been observed for almost all the rivers, with the consequent change in river morphology from braided to single channel. In some cases, streambeds currently lie over the impermeable formations composing the foothills of the northern Apennines [16,17]. As already speculated by [17], this may have caused a deficit in the recharge of the aforementioned aquifers because of the reduced water losses through the streambeds. Third, the slight reduction of precipitations detected in the upper parts of the catchments [18] as well as the land use change (i.e., catchments renaturalization with a subsequent increase in evapotranspiration processes) have led to a reduction in mean annual river flow rates [15]. In turn, this fact causes recharge to groundwater through streambed losses to be remarkably reduced.

Although apical parts of the alluvial fans have always been considered as the main zones for aquifer recharge, quotas from streambed dispersions have never been quantified except with the exclusive use of modeling approaches [4,19,20].

In this work, we present the first attempt to estimate the recharge of these alluvial aquifers by means of an inexpensive direct method (salt tracing tests). We have focused our attention on the alluvial fan of the Tresinaro River, which represents an ideal test site for estimating the streambed dispersion of a river and whose outcomes may also have implications for other case studies worldwide. Here, the river enters the lowlands starting from a clayey streambed allowing us to estimate the runoff of the watercourse before entering the apical part of its alluvial fan. Then, the river flows through its alluvial fan almost exclusively in a single channel permitting the evaluation of flow rates with reduced estimate errors. Moreover, the river is not affected by mining of sands and gravels from the riverbed and has, in the apical part of its alluvial fan, a continuous flow measurement station.

This leads tracing test techniques to be potentially useful in identifying the sectors of the Tresinaro alluvial fan in which the streambed dispersion is larger, as well as trying to quantify the amount of recharge conveyed to the underlying aquifers even at an incontinuous way (by linking the total stream losses to the continuous measurement station).

2. Study Area

2.1. Climatic and Hydrological Settings

The study area is represented by the alluvial fan of the Tresinaro River (Figure 1), which is located at the foothills of the northern Italian Apennines close to the town of Scandiano (Emilia-Romagna region). The altitudes gently decrease toward NE from 150 m a.s.l. to approximately 50 m a.s.l. The authors of [18] provided an overview of the climatic settings of the area by processing a long-term time series of daily precipitations and tem-

peratures from all meteorological stations included in the Emilia-Romagna region. The mean annual rainfall distribution over the period 1990–2015 was approximately 900 mm/y. The rainfall distribution during the year is characterized by two marked positive peaks in autumn and springs seasons, when cumulative amounts may account for 400 mm and 500 mm, respectively (in the summer months precipitations are reduced as well as during the winter ones). Moreover, potential evapotranspiration is particularly active during the summer period (cumulative values of up to 650 mm in the northernmost part of the alluvial fan).

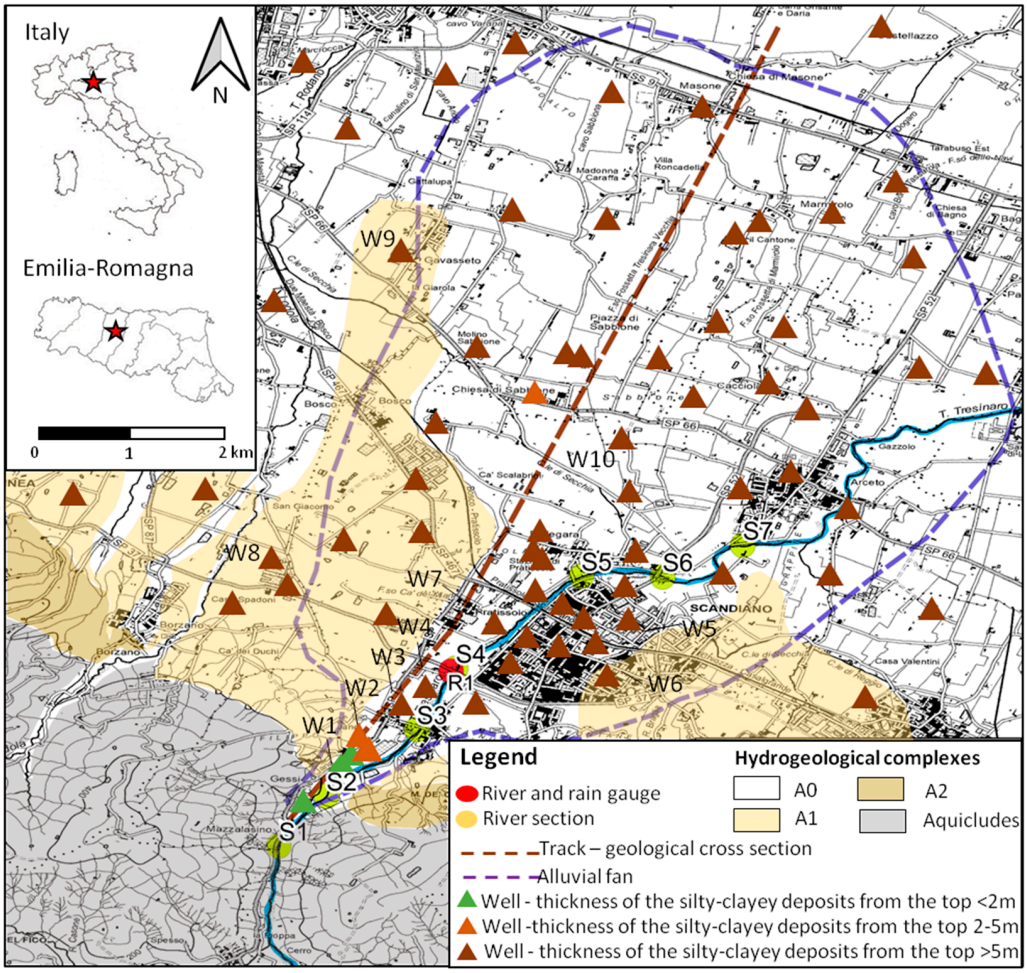

Figure 1. Sketch map of the Tresinaro alluvial fan (dashed purple line) along with river sections in which salt slug injections were carried out (yellow points from S1 to S7), river and rain gauge (red point R1), well within the continuous monitoring of the groundwater level and temperature (green triangle W1) and other wells (coded from W2 to W10) in which a measure of the groundwater level was available (see Supplementary Material Table S1). Locations of the existing wells (from [21]) are added along with the thickness of the poorly permeable silty-clayey deposits (measured from the surface) and the hydrogeological complexes (readers are referred to Section 2.2 for further details). Track line of the simplified hydrogeological cross section (dashed brown line; see Figure 2 for the corresponding cross section) is also reported.

The Tresinaro River originates at about 956 m a.s.l. The discharge starts to be sustained at about 420 m a.s.l., where the confluence with an important group of springs provides up to several hundred L/s to the river (Mulino delle Vene springs, [22]). There are no dams or diversion/branch canals nor sand and gravel mining in the River Tresinaro as far as the start of its alluvial fan. Instrumentation consisting of stream and rain gauges is located a few dozens of meters upstream of Scandiano (R1, see Figure 1) measuring water levels and

precipitations every 15 min for civil protection purposes (flood events). Data have been made available by [23]. The water levels could be converted into discharges by means of a rating curve. Unfortunately, control works after a flood occurred in February 2014, have made the above-mentioned rating curve useless. By considering the period 2003–2014, the Tresinaro river showed perennial discharges with mean annual values between 9 m^3/s (2003) and 40 m^3/s (2005).

In the mountainous part of the catchment, the wide spread of clay-rich sediments and rocks leads river discharge to closely follow the rainfall distribution during the year [24]. This means that the Tresinaro River shows a marked pluvial discharge regime in which low flows take place in the summer–early autumn periods (August, September, and October) with minimum values of discharges that can be in the order of few tens of L/s. Floods usually occur in autumn (October and November) and spring (March and April), with discharge peaks that can be higher than 70 m^3/s. It is worth noting that the time lag of peak discharges after the most extreme precipitation events is usually less than 24 h in these two wet periods.

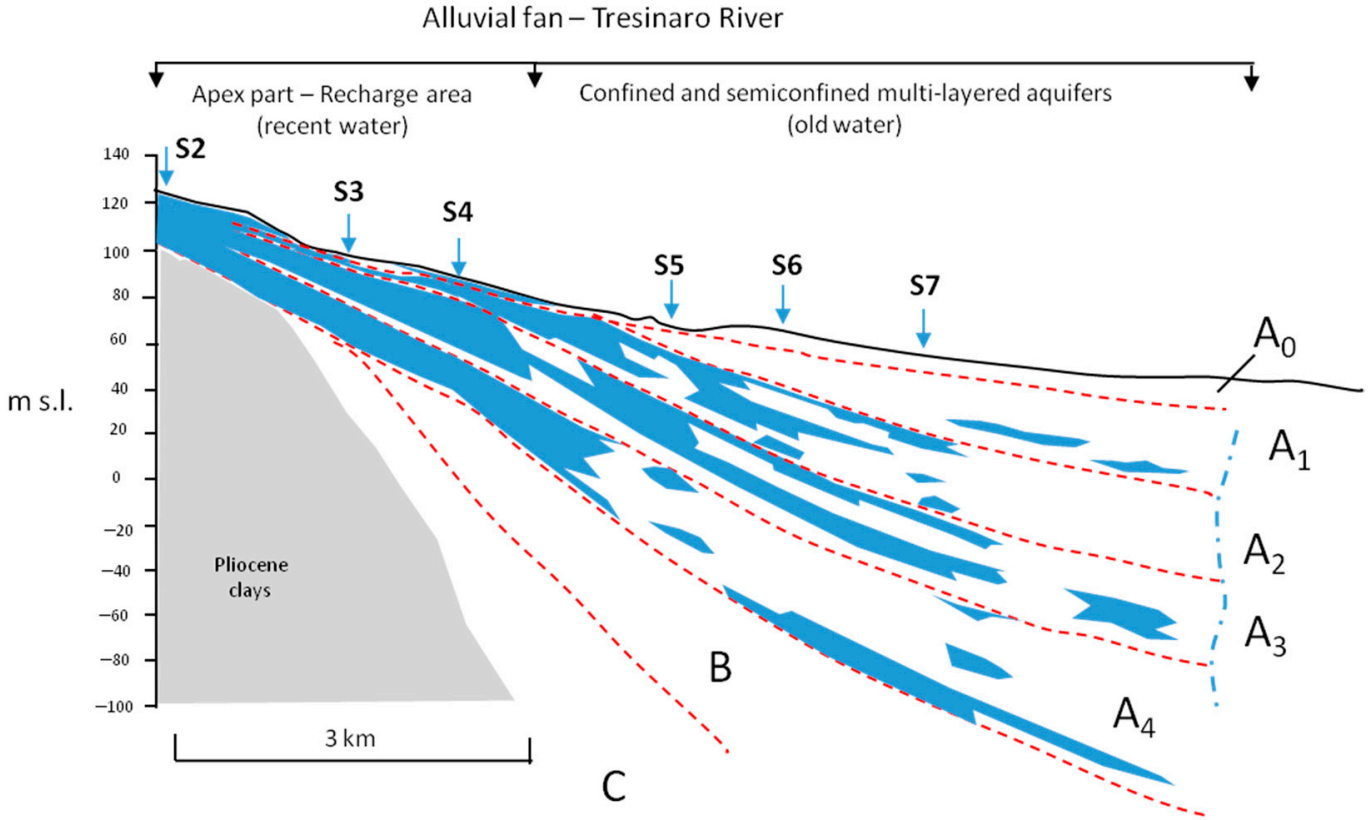

Figure 2. Simplified hydrogeological cross-section of the Tresinaro river alluvial fan along with hydrogeological complexes composing Aquifer Group A (modified after [21,25]; blue parts identify gravels and coarse sand deposits while white ones those areas in which clays and silts are dominant) and river sections in which salt slug injections were carried out (from S2 to S7). Due to a limited number of deep wells, hydrogeological complexes belonging to Aquifer groups B and C are not reported. Readers are referred to Figure 1 for the track line.

2.2. Hydrogeological Features

The alluvial fan of the Tresinaro River started from the inside of the mountain chain and is oriented almost SW–NE. A geological cross-section can be drawn thanks to several wells that were drilled for oil exploration and water supply during the last 70 years over the area and were accompanied by detailed stratigraphic reconstructions (available from [21,25]).

Akin to the other alluvial fans facing the northern Italian Apennines, the alluvial fan of the Tresinaro River has developed over a basal aquiclude made up of overconsolidated

marine clays deposited during the Pliocene (see Figure 2). The alluvial fan is made up of sedimentary particles (grain size ranging from clays to gravels) that were made available by the continuous dismembering of the bedrock forming the mountainous part of the river catchment. The long-term variations in the river discharge and in the sea levels that had occurred during the Pleistocene have implied a change in its solid transport. As a consequence, lenses of gravelly deposits (in form of widespread braided-river sedimentation) have propagated northward (distal parts can be located up to about 10 km from the foothills) in the most humid periods (concurrent to lowstand sea levels of the Adriatic Sea). On the contrary, in the driest periods (concurrent to highstand sea levels of the Adriatic Sea), the coarsest deposits have stopped in the vicinity of the foothills of the northern Apennines and were followed, toward the north, by finer deposits made up of silty-clayey materials (Figure 2). As a result, the alluvial fan is characterized, in the vicinity of the mountain foothills, by an almost undifferentiated gravelly pack (apical part) that, by moving northward, evolves into an overlay of poorly permeable (aquitards and aquicludes composed of clayey and silty materials, or even peats of a swamp environment) and permeable materials (aquifers made up of gravels and sands). With the exception of the initial portion of the apical part closest of the Tresinaro River, the low permeable silty-clayey deposits dominate most of the top-soils of the alluvial fan (see Figure 1, with the overall predominance of wells in which the thickness of silts and clays measured from the surface is greater than 5 m).

Due to the above-mentioned hydrogeological features, the apical part of the alluvial fan acts as a monolayer aquifer hosting unique groundwater whose flow paths move slowly toward the north into compartmentalized groundwater flow systems hosted in several aquifer lenses. The latter have been grouped by [2] into three main Aquifer Groups (namely A, B, C). Aquifer Group A and Aquifer Group B are made up of sediments younger than 450 ka and 650 ka, respectively; Aquifer Group C is much more older (up to 3.9 Ma). All groups are multilayered (as hydrogeological complexes from the top to the bottom of each group; A1 to A4, B1 to B4, C1 to C5) and interconnected in the vicinity of the mountain foothills (apical part of the alluvial fan; see Figure 2). From the hydrogeological point of view, [2] resumed the lithological characteristics of the hydrogeological complexes belonging to Aquifer Group A. Such data were based on a large number boreholes, which in turn confirmed the highest hydraulic conductivity (k) values in the apical part of the fan (maximum k in the order of 8×10^{-3} ms^{-1}) and lower values moving northward (distal part of the fan; minimum k in the order of 10^{-8}–10^{-9} ms^{-1}):

- A0 (aquitard/aquiclude): unconfined or locally semiunconfined aquitard/aquiclude that mainly consists of floodplain filling silts and clays covering the majority of the fan (see Figures 1 and 2). In the apical part of the alluvial fan, lenses of gravels and coarse sands with likely-aquifer behavior. In the middle/distal part of the alluvial fan, lenses of sands and fine sands of reduced extension with the possibility of hosting perched groundwater during the winter and spring months (i.e., unconfined groundwater separated from underlying groundwater in A1 by an unsaturated zone; [25]). Maximum thickness is reached in the distal part of the fan (about 10 m);
- A1: along the Tresinaro River and in the vicinity of the apical part, gravels (channel deposits) amalgamated with the underlying hydrogeological complex A2. In the outcrops at the foothills of the northern Apennines, the hydrogeological complex is dominated by silty clays materials. Toward the distal part of the fan, grain size passes through silty clays with gravelly lenses (interchannel deposits). Lenses of coarse sands can be found in the middle/distal part of fan; their hydraulic interconnection with gravels and coarse sands from the apical part is reduced. Maximum thickness is in the order of 30 m (distal part of the fan);
- A2: coarse gravels in the apical part of the fan with greater prograding northward of the braider-river deposits than the above-mentioned A1. The few outcrops from the hillslope facing the city of Scandiano are composed of fine sands with a silty

matrix. Good interconnection among the coarser lenses along the entire fan (maximum thickness of about 35 m);

- A3: along with A4, it is characterized by the larger longitudinal extension of braided-river deposits with respect to all the other hydrogeological complexes composing the Aquifer Group A. Maximum thickness is 35 m. Medium sands widely outspread also in the middle part of the fan. No outcrops in the study area;
- A4: well-developed aquifer-like behavior up to the middle part of the alluvial fan (maximum thickness is 55 m) with a mixture of sands and gravels. In the distal part of the fan, a sandy aquifer with a remarkable lateral extension is localized at more than 200 m in depth. As in the case of A3, there are no outcrops in the study area.

Groundwater recharge is recognized to be mainly supplied in the apical part of the alluvial fan both by rainfall percolation from the topsoil and the streambed dispersions; as a result, groundwater levels change remarkably during the years (up to more than 3 m in W1, located in the vicinity of S2; see the recharge period focused on February–March 2016 reported in Figure 3 linked to the increased flow rates in the Tresinaro River). In more detail, groundwater level in the vicinity of the S2 (well W1) is at about 119 m a.s.l., while in S3 and S4, it is at 96 m a.s.l. (well W3) and S4 (well W4), respectively. Downstream of the apical part, aquifers (from A1 to the bottom) become multicompartmentalized as they are superimposed to aquitards and aquicludes; there, potentiometric heads change little during the year and are pressurized (groundwater levels close to 80 m a.s.l. in the middle part of the alluvial fan and 68 m a.s.l in the distal part (see W5, W6, and W7 in Supplementary Material S1 as well as [25]).

It should be pointed out that the dynamics of water consumption here are related to both water supply for human purposes (4 water wells located 1 km north of Scandiano are under the control of the local authorities that supply water for more than 35,000 inhabitants at a mean flow rate of 115 L/s from hydrogeological complexes A2 and A3; [26]) and agriculture (dozens of wells whose screens are mainly slotted within Aquifer Group A). With reference to the agriculture, it must be stressed that volumes of groundwater extracted by the wells change greatly from year to year, mainly depending on soil moisture deficits, but are in the order of that for human supply [20]. In case of prolonged dry periods, the groundwater pumping from the aquifers can double, causing generalized decreases of the piezometric levels over the whole alluvial fan, which are more pronounced in the deep and confined aquifers from the distal part.

In the apical part of the alluvial fan, a number of hydrochemical features also indicate direct and fast recharges. First, in the period 2002–2008, several wells were characterized by a relatively high content of nitrates (up to 70 mg/L in the period 2002–2008; [26]). The latter were mainly driven by intensive agriculture practices that occurred in the past (manure spreading and synthetic fertilizer; [9]). Second, as in the case of nitrates, total dissolved solids also change during the year (Ca (Mg)-HCO_3 facies with total dissolved solids (TDS) up to about 500 mg/L in the apical part) with decrements concentrated in the recharge period (from November to April; [27]). Third, the redox potential (E_h) in the groundwater from the apical parts is always high (up to 350 mV), indicating the recent exposure of these water to atmospheric oxygen [28].

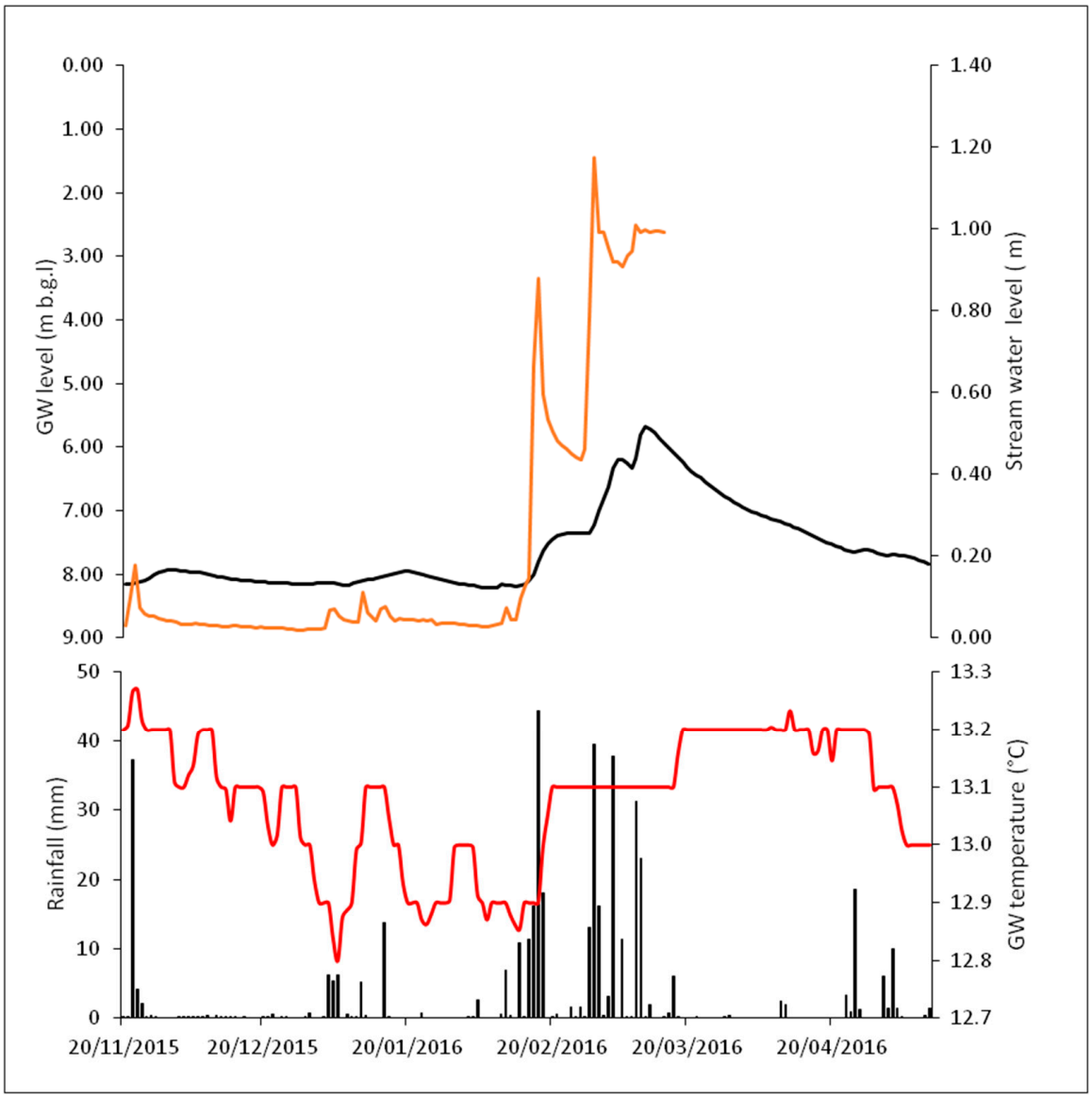

Figure 3. In-continuous daily groundwater levels (dark line) and temperatures (red line) detected in well W from the period 20 November 2015 to 11 May 2016. Daily precipitations (black bar) and stream water level (orange line) from R1 gauge are also reported (readers are referred to Figure 1 for the exact locations of W and R1).

3. Material and Methods

3.1. River Discharge Estimates

In order to assess streambed dispersion along the alluvial fan of the Tresinaro River, 49 river discharges measurements involving seven river sections (from upstream to downstream: S1, S2, S3, S4, S5, S6, S7) were carried out over the period 26 May 2013 to 27 September 2013, a time window in which the river flow rates progressively decrease being almost exclusively fed by the saturated portion of the mountainous aquifers (i.e., recession curve). The above-mentioned 49 rivers discharges measurements were carried out through seven different campaigns (campaign 1: 26 May 2013; campaign 2: 15 June 2013; campaign 3: 22 June 2013; campaign 4: 27 July 2013; campaign 5: 10 August 2013; campaign 6: 15 September 2013; campaign 7: 27 September 2013; see Figure 4).

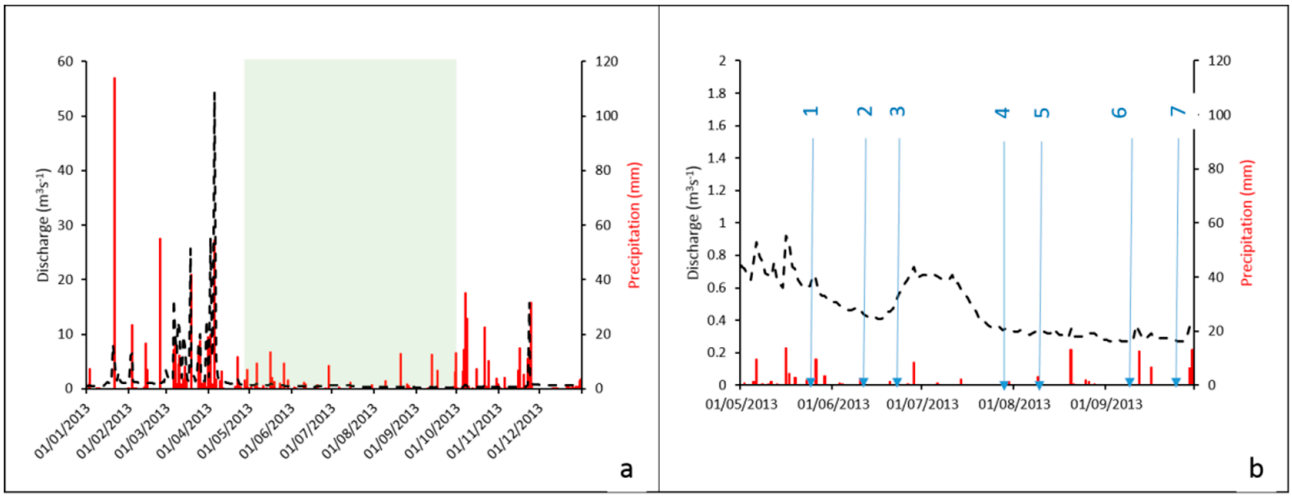

Figure 4. (**a**) Daily discharges (dashed black line) and precipitations (red line) detected in R1 (here, we recall that R1 is located in the same place of section S4) from 1 January 2013 to 31 December 2013. (**b**) Detail of the period from 1 May 2013 to 30 September 2013 in which the seven salt-diluted solution slug injection campaigns were carried out (blue arrows).

Although several techniques for river discharge assessment are available in the literature (readers are referred to [29,30] for a comprehensive review such methods), we selected the artificial method consisting of slug injection of a hyperconcentrated solution (NaCl) for several reasons. First, the irregular shape of the sections coupled with the frequent low water depth make the use of direct measurement methods such as current meters (immersed in different points of a river cross-section to acquire the mean flow velocity) inconvenient. Second, NaCl has been widely used in the literature and is one of the most used chemical tracers in tracing hydrology having almost no (or low) environmental impact [29]. Third, the Tresinaro River at the beginning of its alluvial fan is characterized by low salinity (total dissolved solids less than 500 mg/L during low flow period; [22,31]) while potential sources of NaCl (such as confluence with sewages and purification systems) were not active along the investigated reach of river when slug injections were carried out. This allows a reduced amount of tracer to be used. Fourth, the injection of hyperconcentrated NaCl solution in the event of water columns with a reduced content of suspended materials (i.e., clays) permits high precision in discharge estimates [30].

With reference to this last point, it must be recalled that low content of suspended materials in water column is pivotal as the discharge assessment by the salt-tracing technique is based on the integration method proposed by [32]. This method requires the slug injection of a solution with a known tracer content into the river and the subsequent determination of the tracer concentration downstream by means of a conductivity probe. From a mathematical point of view, if we consider Q as the river discharge, the initial concentration of salt in the river water C_0 (in the section where conductivity probe is placed) can be written as follows:

$$C_0 = Q \int_0^\infty c dt \quad (1)$$

During a given time range, T, which is equal to the time needed for the tracer to be transported downstream, an average value for the sample is found by sampling the tracer concentration present in the measurement station at regular time intervals.

Then:

$$\int_0^\infty c dt = \bar{c}\, T \quad (2)$$

Finally, the discharge is calculated as:

$$Q = \frac{c_0}{c} \frac{V}{T} \quad (3)$$

where c is the concentration of the sample in volume V.

The main assumption of this method is that all the injected amount of tracer must be detected by the conductivity probe. Since suspended sediments in the water column induce sodium adsorption, river water with high turbidity (such as those characterizing the Tresinaro River after intense rainfall events) is characterized by larger error estimates. For these reasons, our campaigns were focused on the period of recession of the river flow-rates, i.e., when the waters were almost free of suspended sediments.

In order to find the proper amount of salt to be diluted into the water, at the campaign 1, and for the only river section S7, a preliminary set of tracing tests were performed by testing the amount of tracer (in the form of hyperconcentrated solution with larger amounts of NaCl) in the river. We started from the assumption that the average tracer concentration should be 10 times higher than the detection limit of the tracer itself [31]. The first trial used the smallest quantity of salt (100 g in 5 L of water) while the subsequent ones tested progressive increase of salt up to 700 g in 5 L of water (namely 200 g, 300 g, 500 g, and 700 g). Each trial was repeated four times in order to estimate mean value and the corresponding uncertainties (as $\pm 2\sigma$) for each amount of tracer. Conductivity was measured in-continuous 100 m downstream of the injection point by using a conductivity probe (STS DL/70/N MULTI); the acquisition time was set at 6 s while precisions of such instrumentations are reported as equal to 2%. It is worth noting that the 100 m distance was selected following the results by [22] for the same river to allow a well mixing between river flow paths and the hyperconcentrated solution. Data were processed on-site for detecting the most useful amount of tracer to be used also for slug injections in the other river sections in campaign.

All of the slug injections were carried out by going upstream (i.e., starting from S7 to S1) to avoid cross-contamination phenomena among the measures carried out in the several sections. In detail, all the sections were selected to ensure constant and permanent flow regimes along the 100 m between injection points and locations where conductivity probes were placed (i.e., no pools or backwater areas were present), while changes in flows are considered negligible. S1 was selected several tens of meters prior to the beginning of the apical part of the alluvial fan; here, the riverbed is imposed on clayshales, hence, no subsurface seepage was possible allowing the effective river discharges at each campaign to be assessed before any streambed loss.

3.2. Streambed Losses Assessment

The streambed loss from each reach of river identified by two subsequent sections was assessed by subtracting the corresponding discharge values obtained as anticipated in Section 3.1. The calculation is affected by uncertainties related to each discharge value (preliminary estimated through salt slug injection method); thus, the final errors associated to streambed losses were assessed using the common error propagation methods reported in [33]. As an example, and with reference to a specific campaign, if discharges from Section 1 (Q_{S1}) and Section 2 (Q_{S2}) were obtained along with the corresponding $\pm 2\sigma$ uncertainties (here, renamed as $\pm dQ_{S1}$ and $\pm dQ_{S2}$, respectively), the corresponding errors $\pm dQ_{S1-S2}$ associated to streambed loss Q_{S1-S2} were calculated as follows:

$$dQ_{S1-S2} = \sqrt{dQ_{S1} + dQ_{S2}} \quad (4)$$

The acquisition of discharges from the seven campaigns permitted the development of an interpolation model linking the discharge at the beginning of the alluvial fan to the total streambed losses. In this way, total stream losses along the alluvial fan can be assessed whenever a value of discharge from S1 is available. The interpolation linear regression (ordinary least squares OLS model; see [34] for further detail) was selected after a goodness-of-fit comparison and error bounds corresponding to a 95% confidence interval ($\pm 2\sigma$) were added. It must be stressed that the basic assumption of linear regression is that data are time-invariant (i.e., stationary). Thus, the presence of outliers or heteroscedasticity (i.e., modeling errors have not the same variance over the alignment) or autocorrelation lead the assumption of stationary to be violated; thus, slopes and intercepts from linear regression

may not be meaningful. In this work, we exploited conventional statistical tests for verifying normality (i.e., presence of outliers inducing non-normality; Doornik-Hansen test [35]) heteroscedasticity (Breusch-Pagan test [36]) and autocorrelation (Durbin–Watson [37]). All of the above-mentioned tests are based on a comparison of the corresponding statistics' p-values results with a threshold value (level of significance α set at 0.01) to decide whether the null hypotheses have to be rejected ($p < 0.01$) or not ($p > 0.01$). The following null hypotheses were selected: normality (Doornik–Hansen), homoscedasticity (Breusch–Pagan), no autocorrelation (at a lag of 1) in the residuals (Durbin–Watson).

4. Results

Tracing tests carried out in section S7 during campaign 1 and using different amounts of tracers (here, we recall that we used the following quantities of salt for preparing hyperconcentrated solutions: 100 g, 200 g, 300 g, 500 g, 700 g) were obtained as per formula 3 and summed up in Table 1. Results indicated that tests carried out using 200 g and 300 g of NaCl provided the closest results (98 and 94 ls^{-1}, respectively) as well as their reliability (2σ obtained as per formula 4 and equal to 3.3% and 4.1%, respectively; corresponding variances of ± 4 ls^{-1} and ± 7 ls^{-1}). These errors were in the order of those reported by [30] (about 3%) and [38,39] (4%–7%) for equivalent tests carried out in rivers from Italy and New Zealand.

Table 1. Discharges (in ls^{-1} along with the corresponding uncertainties equal to $\pm 2\sigma$) as result of the salt injections tests carried out during campaign 1 at Station S7.

Longitude (*X*)	Latitude (*Y*)	Station Code (Discharge Code)	Number of Tests	Amount of Tracer (g) in 5 L of Water	Station Code	Discharge ls^{-1}	Errors (2 σ; %)	Errors (2 σ; ls^{-1})
10°42′51.69″ E	44°36′42.85″ N	S7	4	700	S7	111	±12.8	±15
10°42′51.69″ E	44°36′42.85″ N	S7	4	400	S7	102	±6.3	±6
10°42′51.69″ E	44°36′42.85″ N	S7	4	300	S7	94	±4.1	±4
10°42′51.69″ E	44°36′42.85″ N	S7(Q_{S7})	4	200	S7	98	±3.3	±3
10°42′51.69″ E	44°36′42.85″ N	S7	4	100	S7	76	±8.9	±7

Thus, errors being slightly reduced for solution of 200 g of salt diluted into 5 L of water, we used 200 g diluted in 5 L of water for all the remaining tests.

Results were reported in Table 2 along with the corresponding uncertainties ($\pm 2\sigma$). Discharges ranged between 324 ± 11 ls^{-1} (S1 in campaign 1) to 21 ± 1 ls^{-1} (S7 in campaign 7). Except for the campaign 3, a slight decrease of discharges was observed for all river sections from campaign 1 to campaign 7. Moreover, and without differences between the different campaigns, the highest discharge values always characterized S1 whereas river flow rates decreased from S1 to S5. On the contrary, river flow rates were substantially constant or even increasing by going from S5 to S7. This fact allowed to identify a specific river reach in which stream losses toward underlying aquifers were active, i.e., the reach of river included between S1 to S5 (for a total length of approximately 4800 m out of the investigated 6850 m).

Table 2. Discharges (in ls^{-1} along with the corresponding uncertainties calculated as $\pm 2\sigma$) as result of the salt injection tests. Amount of salt used for preparing hyperconcentrated solutions were always 200 gl^{-1} in 5 L of water. Values used as *x*-axis for obtaining regression line in Figure 5 are highlighted in bold.

Longitude (*X*)	Latitude (*Y*)	Progressive Distance from S1 (in m)	Station Code (Discharge Code)	Campaign						
				1	2	3	4	5	6	7
				Discharge (ls^{-1})	Discharge (ls^{-1})	Discharge (ls^{-1})	Discharge (ls^{-1})	Discharge (ls^{-1})	Discharge (ls^{-1})	Discharge (ls^{-1})
10°42′51.69″ E	44°36′42.85″ N	6868	S7 (Q_{S7})	98 ± 3	99 ± 3	97 ± 3	68 ± 2	34 ± 1	43 ± 1	21 ± 1
10°42′17.09″ E	44°36′27.55″ N	5740	S6 (Q_{S6})	99 ± 3	103 ± 3	96 ± 3	70 ± 2	35 ± 1	46 ± 1	35 ± 1
10°41′35.25″ E	44°36′27.18″ N	4804	S5 (Q_{S5})	95 ± 3	98 ± 3	95 ± 3	72 ± 2	35 ± 1	45 ± 1	38 ± 1
10°40′39.55″ E	44°35′46.54″ N	3039	S4 (Q_{S4})	104 ± 3	103 ± 3	106 ± 3	69 ± 2	48 ± 2	47 ± 2	37 ± 1
10°40′21.38″ E	44°35′20.29″ N	2116	S3 (Q_{S3})	156 ± 5	144 ± 5	154 ± 5	86 ± 3	58 ± 2	76 ± 3	57 ± 2
10°39′31.58″ E	44°34′42.16″ N	456	S2 (Q_{S2})	253 ± 8	162 ± 5	224 ± 7	109 ± 4	81 ± 3	94 ± 3	73 ± 2
10°39′11.50″ E	44°34′18.91″ N	0	S1 (Q_{S1})	**324 ± 11**	**214 ± 7**	**270 ± 9**	**154 ± 5**	**122 ± 4**	**104 ± 3**	**84 ± 3**

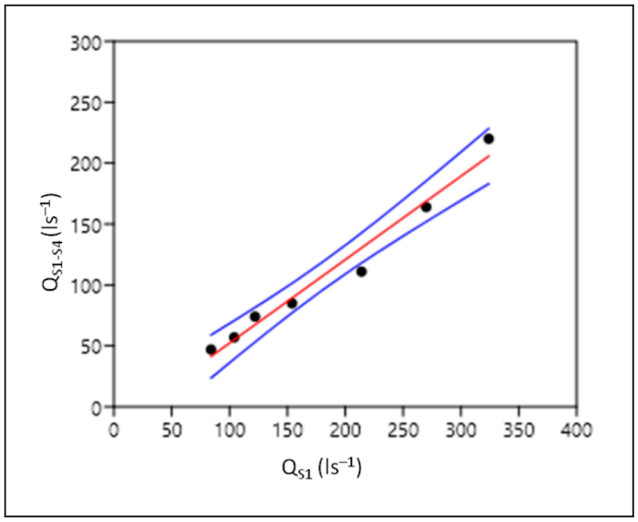

Figure 5. Linear regression (or rating line; red continuous line) linking discharges at S1 (Q_{S1}) to total stream losses along the alluvial fan ($Q_{S1–S4}$). Error bounds (blue continuous lines) corresponding to the 95% confidence intervals are also reported.

Table 3 reports the losses from the streambed obtained by subtracting the discharge values from subsequent sections. We specified that some negative values (i.e., reduced increment of discharge close to the errors of the estimates) occurring in the river reach S5–S6 have been forced to 0 due to presence of some drainpipes conveying treated and untreated wastewater (quantifiable in a couple of ls^{-1}) from industrial and human activities in Scandiano. Neither the amount of wastewater from pipes was quantified on site nor their functionality as in most cases their exits are located directly in the riverbed. It can be noted that most of the water losses occurred in the reach between sections S1 and S4, with evident peaks of streambed losses in reach S1–S2 (up to 71 ± 14 ls^{-1} in campaign 1 equivalent to 156 ± 30 ls^{-1}km^{-1}) and reach S3–S4 (highest value of 52 ± 6 ls^{-1} in campaign 1 equivalent to 56 ± 7 ls^{-1}km^{-1}) while there is a significant decrease in reach S2–S3 (losses between 58 ± 6 ls^{-1}km^{-1} in campaign 1 to 10 ± 2 ls^{-1}km^{-1}).

Table 3. Losses from streambed (in ls^{-1} and ls^{-1} km^{-1} along with the corresponding uncertainties calculated with the error propagation method presented by [33]). The losses from streambed that have been forced to 0 are in italics.

Losses from Streambed as per River Reach (Distance between Subsequent Sections in m)	Campaign 1 (Stream Losses)		Campaign 2 (Stream Losses)		Campaign 3 (Stream Losses)		Campaign 4 (Stream Losses)		Campaign 5 (Stream Losses)		Campaign 6 (Stream Losses)		Campaign 7 (Stream Losses)	
	(ls^{-1})	(ls^{-1} km^{-1})	(ls^{-1})	(ls^{-1} km^{-1})	(ls^{-1})	(ls^{-1} km^{-1})	(ls^{-1})	(ls^{-1} km^{-1})	(ls^{-1})	(ls^{-1} km^{-1})	(ls^{-1})	(ls^{-1} km^{-1})	(ls^{-1})	(ls^{-1} km^{-1})
$Q_{S6–S7}$ (1128 m)	1 ± 5	1 ± 4	4 ± 2	4 ± 4	*0*	*0*	2 ± 3	2 ± 3	1 ± 2	1 ± 1	3 ± 1	3 ± 2	14 ± 2	12 ± 2
$Q_{S5–S6}$ (936 m)	*0*	*0*	*0*	*0*	*0*	*0*	4 ± 3	2 ± 4	0	0	*0*	*0*	3 ± 2	3 ± 1
$Q_{S4–S5}$ (1765 m)	9 ± 5	5 ± 3	5 ± 5	3 ± 3	6 ± 5	6 ± 3	*0*	*0*	7 ± 2	7 ± 1	1 ± 2	1 ± 1	*0*	*0*
$Q_{S3–S4}$ (923 m)	52 ± 6	56 ± 7	41 ± 6	44 ± 6	48 ± 6	52 ± 7	17 ± 4	18 ± 5	11 ± 2	11 ± 3	31 ± 2	31 ± 3	20 ± 2	22 ± 2
$Q_{S2–S3}$ (1660 m)	97 ± 10	58 ± 6	18 ± 7	11 ± 4	70 ± 9	42 ± 5	23 ± 5	14 ± 3	14 ± 3	14 ± 2	11 ± 3	11 ± 2	16 ± 4	10 ± 2
$Q_{S1–S2}$ (456 m)	71 ± 14	156 ± 30	52 ± 9	114 ± 19	46 ± 12	101 ± 25	45 ± 6	99 ± 14	41 ± 5	90 ± 11	10 ± 4	22 ± 10	11 ± 5	24 ± 8

This fact (decrease of stream losses in reach S2–S3) could be due to the presence of clogging taking place for several dozens of meters upstream of a river dam. An important increase in stream losses in the reach S2–S3 was observed in Campaign 3 (42 ± 5 ls^{-1}km^{-1}) and provided further confirmations of the presence of clogging. In fact, Campaign 3 was carried out during the rising limb of a reduced peak flow (see Figure 4b) that may have promoted the removal of the finest sediment (clays and silts) clogging the streambed.

Table 4 sums up losses from streambed starting from river sections S1 to S5. As mentioned above, almost all of the losses toward the underlying aquifers (i.e., total stream losses $Q_{S1–S4}$) occurred between S1 and S4.

Table 4. Losses from streambed (in ls^{-1} along with the corresponding uncertainties calculated with the error propagation method presented by [33]). Values used as *y*-axis (i.e., total stream losses) for obtaining regression line in Figure 5 are highlighted in bold.

Incremental Stream Losses from S1 (Distances between Sections)	Campaign 1	Campaign 2	Campaign 3	Campaign 4	Campaign 5	Campaign 6	Campaign 7
$Q_{S1–S5}$ (4804)	229 ± 11	116 ± 8	175 ± 9	/	87 ± 4	59 ± 4	/
$Q_{S1–S4}$ (3039)	**220 ± 11**	**111 ± 8**	**164 ± 10**	**85 ± 6**	**74 ± 4**	**57 ± 4**	**47 ± 3**
$Q_{S1–S3}$ (2116)	168 ± 12	70 ± 9	116 ± 10	68 ± 6	64 ± 4	28 ± 4	27 ± 3
$Q_{S1–S2}$ (456)	71 ± 14	52 ± 9	46 ± 12	45 ± 6	41 ± 5	10 ± 5	11 ± 4

In detail, total stream losses were between 220 ± 11 ls^{-1} (Campaign 1) to 47 ± 3 ls^{-1} (Campaign 7). In the $Q_{S1–S4}$–Q_{S1} plot (see Figure 5), dots lie on a straight line (see red line in Figure 5 as well as blue continuous lines corresponding to the 95% confidence intervals) that can be obtained through OLS regression (as reported in Section 3.2). This regression line is characterized by the following equation:

$$Q_{S1-S4} = 0.69Q_{S1} - 16.9 \quad (5)$$

with coefficient of determination (R^2) and *p*-value equal to 0.97 and 0.00005, respectively. Assumptions underlying the OLS linear regression are respected as all the three tests (namely Breusch–Pagan, Doornik–Hansen, Durbin–Watson; see Section 3.1) were characterized by *p*-values higher than the selected threshold (α = 0.01; here, we recall that *p*-values higher than α confirm that null hypotheses have to not be rejected). In detail, there were no changes in variance along the alignment (i.e., homoscedasticity; Breusch–Pagan test with p = 0.58) and no autocorrelation (at a lag of 1) in the residual (Durbin–Watson test with p = 0.83). Furthermore, no point in the alignment represented an outlier as normality was confirmed (Doornik–Hansen tests with p = 0.20).

5. Discussion

5.1. Streambed Dispersions and Relationships with Hydrogeological Features

The 49 slug injection tests have allowed us to clarify that almost all of the losses towards the underlying aquifers (i.e., total stream losses $Q_{S1–S4}$) take place in a river reach between S1 and S4. As clearly visible in Figure 2, the sector of river starting few tens of meters northward of S1 and ending in S4 lies over the apical part of the alluvial fan, where coarser deposits (gravels and sands) are directly connected to the streambed. A hundred of meters downstream of S4, the streambed of the Tresinaro rivers lost its connection with the underlying aquifers being imposed into the silty and clayey deposits of the hydrogeological complex A0. There, we recall that also the terraces alongside the main channel of river included between S2 and S4 are made up of a thick cohesive deposit of A0 (thickness of more than 5 m; see wells W3 and W4 in Figure 1) that do not promote rainfall percolation from the topsoils (see also [25]. The latter is enhanced in a reduced area (<0.7 km^2) upstream of S2, where the thickness of the above-mentioned deposits of A0 is reduced or even nonexistent (see wells W2 and W1 in Figure 1). Thus, the majority of the recharge of the aquifers belonging to the alluvial fan is driven by streambed dispersion.

Moreover, unlike what we would have expected, we found that streambed dispersion is not constant over the apical part of the alluvial fan nor characterized by a progressive decrease going downstream. In fact, a significant decrease of streambed dispersion always affects reach S2–S3 if compared with the subsequent reach S3–S4. Such a fact may be related to a river dam located in S3.

As mentioned in Section 4, it has been observed during the field activities that gravels and sands of the streambed were clogged by the sedimentation of finest sediments (clays and silts) for a 50 m long sector of river upstream from the river dam. We believe that such clogging does not characterize all the hydrologic year as clays and silts are removed during

the rising ling of peak flow events. Such fact may enhance the streambed dispersion when river discharge is rising up to the peak flow; during the falling limb after the peak, and in particular when velocity of the current is lower than that necessary to keep clays and silts suspended, the streambed dispersion results furthermore hampered. Downstream of S4, we found evidence of intermittent recharge (even with low flow rates; see Table 3) toward the underlying aquifers that should be focused at the beginning of reach S4–S5, where streambed still lies over the aquifer-like deposits of A0 (see Figure 2). Going downstream of S5, no streambed losses were identified during the seven different campaigns as, in some cases, discharges values slightly increase (even if losses from streambed per river reaches between S5 and S7 were often included in the estimate errors; see Table 4). Being a potentiometric surface there at about 15 m below ground level and slug injection campaigns carried out during summer periods, we believe that such reduced increments of discharges downstream of S5 have to be linked to draining pipes conveying treated and untreated wastewater from the purifiers of Scandiano. Nonetheless, and as already highlighted in Section 2.2, the presence of perched groundwater during the winter–spring months is confirmed [25]. The latter are hosted in reduced lenses of sands and fine sands from A0 and may feed the river discharge with flow rates in the order of few ls^{-1} when intersected by the river course.

By exploiting the groundwater levels data (see Supplementary Materials, Table S1) involving the water wells alongside the Tresinaro River (i.e., W1, W2, W3, W4, W5), a first approximation the water table below the stream course can be obtained and further evidence of the different streambed dispersion rates is provided above. The first reach S1–S2 is characterized by the highest hydraulic gradient (0.015), which progressively decreases downstream (0.011 in reach S2–S3; 0.009 in reach S3–S4 and 0.004 in reach S4–S5; about 0.000008 northward). These data confirm the presence of a remarkable groundwater ridge below the river reach of river between S1 and S4 that is recharged continuously by streambed dispersion with the highest rates during flood events.

5.2. Overall Considerations on the Tested Approach: In-Continuous Recharge Assessment and Possible Implications for Other Case Studies

It is evident that such approach can be usable in other alluvial fans facing the northern Italian Apennines and, more in general, whenever rivers entering the lowlands start to release a quota of their discharges to the underlying aquifers. In particular, the aforementioned results demonstrated the effectiveness in carrying out NaCl slug injections for identifying river reaches along which stream losses are promoted as well as quantifying the total amount of water recharging the underlying aquifers with reduced errors in estimates.

Moreover, once total stream losses have been quantified for a proper number of times, groundwater river recharge can be monitored in real time if a permanent measurement device (such as the common telemetry used for river discharge monitoring) is installed before the alluvial fan starts (in the case of the Tresinaro River, the current instrumentation shall be replaced in S1 as the current location R1 falls within an area in which dispersion is almost inactive).

The usefulness of such results is twofold. First, defining river reaches in which stream losses are promoted helps planning of draining pipes conveying treated and/or untreated wastewater (as well as storm water runoff from streets and service areas) to river in order to avoid any qualitative impact to groundwater. With reference to the Tresinaro river, such confluences should be placed downstream of section S5. Furthermore, all civil settlements and/or industrial activities and the corresponding purifiers located in the mountainous sector of the Tresinaro catchment should be suitably designed in order to avoid high concentrations of pollutants which then, starting from the apical part of the alluvial fan, could be conveyed into the porous aquifers. It must be highlighted that some confined aquifers from the alluvial fan of the Tresinaro River have already experienced pollution phenomena in the last decades. Among the most serious case, tetrachloroethylene (a toxic chlorocarbon used for dry cleaning of fabrics that in groundwater behaves as dense nonaqueous liquid phase) was found in the water pumped from several wells. Although the

source of the pollution has not been recognized yet, it is plausible that tetrachloroethylene had been released into aquifers through stream losses.

Second, and as already stated in the Introduction, aquifers hosted in the alluvial fans are currently facing climate change and are subjected to large withdrawals for both aqueduct and agricultural uses which have led to a lowering of the piezometric surface; hence, it is important to continuously monitor stream losses recharging these aquifers to calibrate in advance the volumes of water that can be pumped without altering the qualitative status and quantitative balance of the groundwater resources.

Although such an approach has allowed us to characterize and in-continuous quantify the quota of recharge linked to stream losses, the other quota due to zenithal infiltration from precipitation should be added. In the case of Tresinaro alluvial fan, the amount of recharge provided by zenithal infiltration has already been confirmed as secondary if compared to that of riverbed dispersion ([25]). Being affected by significant alterations of the channel morphologies in the apical part of the alluvial fans (with current streambed laying on impermeable formations), several other rivers outflowing from the northern Italian Apennines are characterized by a prevalent recharge made by zenithal infiltration [5]. In such a case, the splitting of the two recharge quotas (i.e., zenithal precipitation and stream losses) is particularly difficult since increases in river discharges usually occur a few hours after rain events (due to the wide outcrop of impermeable material in the mountainous part of the catchment). As already reported in [5], a possible way to quantify each component should be based on in-continuous monitoring network involving both river discharge, precipitations and groundwater. With reference to groundwater, instrumentation must be able to collect both groundwater levels and some selected physical–chemical parameters (such as TDS and temperature). Such an approach will first have to be tested at each recharge event to differentiate those related to the recharge by stream dispersion alone (river flood generated by rainfall in the upper part of the catchments) from those due to zenithal recharge by precipitation alone (occurring only on the apical part of the alluvial fan and with river fed by base flow).

Furthermore, the implementation of an in-continuous monitoring network would pose the foundation for the application of a suite of environmental tracers (such as isotopes of water) to be obtained at the event scale (that of flood and or rainfall with, at least, hourly sampling activities). This allows end-member mixing analysis to be carried out at the event scale, and aquifer recharge quotas from each component to be better constrained (see, for instance, the recent paper by [40], which exploited the same approach for depicting three end-members feeding a pumping well located in an alluvial aquifer in France).

6. Conclusions

This study has demonstrated that developing an appropriate number of NaCl slug injections in rivers characterized by stream losses represents a valid and inexpensive approach for defining reaches in which groundwater recharge is promoted and to quantify the amount (and the corresponding uncertainties) of stream water conveyed to the underlying aquifers. With reference to the proposed case study (the Tresinaro River and its alluvial fan facing the northern Italian Apennines), results of 49 NaCl slug injections carried out over seven campaigns indicated that the apical part of the alluvial fan is characterized by the highest values of stream losses (up to 156 $\pm$ 30 ls^{-1} km^{-1} in the reach of river between S1 and S2), whose values decreased almost progressively down to nil at about 3 km downstream of S1. Moreover, we found that total stream losses were directly proportional to river flow rates at the beginning of the alluvial fan. This fact allowed us to build a rating line linking river discharge at the beginning of the alluvial fan to the total stream losses; in this way, the placement of a permanent measurement device aimed at continuously monitoring river discharge in S1 would also provide the recharge conveyed to the underlying aquifers.

This information is needed by stakeholders in charge of surface and groundwater management for further adaptation plans, among others (i) placing reaches downstream of

the river, characterized by streambed dispersion the conveying of treated and/or untreated wastewater (as well as storm water runoff from streets and service areas); (ii) developing mitigation measures aimed at reducing the risk of pollutant spills in all civil settlements and/or industrial activities from the mountainous sector of the catchment as well as improving the corresponding purifiers; (iii) development of agricultural best practices capable of inducing an increase in groundwater levels and water quality; (iv) contrasting the overall lowering of the piezometric surface (due to both climate change and withdrawals) by calibrating the volumes of water that can be pumped to the in-continuous monitoring of total stream losses, without altering the qualitative status and quantitative balance of the groundwater resources.

This approach, aiming at evaluating the percentage of aquifer recharge due to stream losses, must be coupled to the classical assessment of the zenithal infiltration, as the majority of rivers flowing out of the mountainous zones toward plains are affected by huge recharge from precipitations. This in-continuous monitoring network should thus also comprise rainfall amount, evapotranspiration, surface discharge, and groundwater. In this context, salt-tracing tests are a rapid and valid tool that can integrate knowledge and provide additional information about the groundwater balance.

Supplementary Materials: The following are available online at https://www.mdpi.com/article/10.3390/hydrology8030118/s1, Table S1: Groundwater level from wells numbered from W2 to W10.

Author Contributions: Conceptualization, F.C.; methodology, F.C. and A.T.; formal analysis, F.C.; writing—original draft preparation, F.C.; writing—review and editing, F.C. and A.T. All authors have read and agreed to the published version of the manuscript.

Funding: This research received no external funding.

Data Availability Statement: The data presented in this study are made freely available thorough Tables 2–4.

Acknowledgments: An early draft of the manuscript has benefited from the valuable suggestions made by three anonymous reviewers.

Conflicts of Interest: The authors declare no conflict of interest.

References

1. Chahoud, A.; Cristofori, D. *Il Le Pressioni Antropiche in Relazione Alle Acque Sotterranee: I Prelievi*; Quaderni di Tecniche di Protezione Ambientale, 85 Pitagora Editrice: Bologna, Italy, 2014; pp. 87–94.
2. Benelli, F.; Pignone, R.; Di Dio, G. *Riserve Idriche Sotterranee della Regione Emilia-Romagna*; SELCA: Firenze, Italy, 2014; p. 120.
3. Farina, M.; Marcaccio, M. *Lo Stato Qualitativo Delle Acque Sotterranee*; 85 Pitagora Editrice: Bologna, Italy, 2014; pp. 57–75.
4. Di Dio, G. Modelling groundwater-stream water interactions in the Taro river hydrogeological basin (western Emilia-Romagna region, northern Italy). *Ital. J. Eng. Geol. Environ.* **2012**, *12*, 23–39.
5. Martinelli, G.; Dadomo, A.; Cervi, F. An Attempt to Characterize the Recharge of Alluvial Fans Facing the Northern Italian Apennines: Indications from Water Stable Isotopes. *Water* **2020**, *12*, 1561. [CrossRef]
6. Martinelli, G.; Minissale, A.; Verrucchi, C. Geochemistry of heavily exploited aquifers in the Emilia-Romagna region (Po valley, northern Italy). *Environ. Geol.* **1998**, *36*, 195–206. [CrossRef]
7. Cervi, F.; Corsini, A.; Marcaccio, M. Confronto tra metodo euristico SINTACS e SINTACS-Woe in base alla distribuzione dell'inquinamento da nitrati-caso studio della conoide del Fiume Enza. In *Esperienze e Prospettive nel Monitoraggio delle Acque Sotterranee: Il Contributo dell'Emilia-Romagna*; Quaderni di Tecniche di Protezione Ambientale, 85 Pitagora Editrice: Bologna, Italy, 2014; pp. 140–147.
8. Tagliavini, S.; Perego, S.; Zontini, S. *Carta Della Vulnerabilità All'inquinamento Degli Acquiferi Della Conoide del Fiume Enza*; Note illustrative. Quad. Tecniche Protezione Ambientale, 11. Studi Sulla Vulnerabilità Degli Aquiferi, 1: 15-51; 85 Pitagora Editrice: Bologna, Italy, 1990.
9. Martinelli, G.; Dadomo, A.; De Luca, D.A.; Mazzola, M.; Lasagna, M.; Pennisi, M.; Pilla, G. Nitrate sources, accumulation and reduction in groundwater from Northern Italy: Highlights provided by a nitrate and boron isotopic database. *Appl. Geochem.* **2018**, *91*, 23–35. [CrossRef]
10. Zanini, A.; Petrella, E.; Sanangelantoni, A.M.; Angelo, L.; Ventosi, B.; Viani, L.; Rizzo, P.; Remelli, S.; Bartoli, M.; Bolpagni, R.; et al. Groundwater characterization from an ecological and human perspective: An interdisciplinary approach in the Functional Urban Area of Parma, Italy. *Rend. Lincei. Sci. Fis. Nat.* **2019**, *30*, 93–108. [CrossRef]

11. Anselmi, M.; Renoldi, F.; Alberti, L. Analytical and numerical methods for a preliminary assessment of the remediation time of Pump and Treat system. *Water* **2020**, *12*, 2850. [CrossRef]
12. Modoni, G.; Darini, G.; Spacagna, R.L.; Saroli, M.; Russo, G.; Croce, P. Spatial analysis of land subsidence induced by groundwater withdrawal. *Eng. Geol.* **2013**, *167*, 59–71. [CrossRef]
13. Bitelli, G.; Bonsignore, F.; Conte, S.D.; Franci, F.; Lambertini, A.; Novali, F.; Severi, P.; Vittuari, L. Updating the subsidence map of Emilia-Romagna region (Italy) by integration of SAR interferometry and GNSS time series: The 2011–2016 period. *Proc. Int. Assoc. Hydrol. Sci.* **2020**, *382*, 39–44. [CrossRef]
14. Preciso, E.; Salemi, E.; Billi, P. Land use changes, torrent control works and sediment mining: Effects on channel morphology and sediment flux, case study of the Reno River (Northern Italy). *Hydrol. Proc.* **2012**, *26*, 1134–1148. [CrossRef]
15. Pavanelli, D.; Cavazza, C.; Lavrnić, S.; Toscano, A. The long-term effects of land use and climate changes on the hydro-morphology of the Reno river catchment (Northern Italy). *Water* **2019**, *11*, 1831. [CrossRef]
16. Bonazzi, U. Modificazioni d'alveo del fiume Secchia avvenute negli ultimi cento anni nei dintorni di Sassuolo (Modena). *Atti Soc. Nat. E Mat. Modena* **1996**, *127*, 67–99.
17. Pellegrini, M.; Tosatti, G. Engineering geology, geotechnics and hydrogeology in environmental management: Northern Italian experiences. In *Geomechanics and Water Engineering in Environmental Management*; Taylor and Francis: London, UK, 1992; pp. 407–428.
18. Cervi, F.; Nistor, M.M. High resolution of water availability for Emilia-Romagna region over 1961–2015. *Adv. Meteorol.* **2018**, *2018*, 2489758. [CrossRef]
19. Chahoud, A.; Gelati, L.; Palumbo, A.; Patrizi, G.; Pellegrino, I.; Zaccanti, G. Groundwater flow model management and case studies in Emilia-Romagna (Italy). *Acque Sotter. Ital. J. Groundw.* **2013**, *2*, 59–73. [CrossRef]
20. Chahoud, A.; Patrizi, G.; Zazzanti, G.; Gelati, L. Il modello di flusso delle acque sotterranee della Regione Emilia-Romagna. In *Esperienze e Prospettive nel Monitoraggio delle Acque Sotterranee: Il Contributo dell'Emilia-Romagna*; Quaderni di Tecniche di Protezione Ambientale, 85 Pitagora Editrice: Bologna, Italy, 2014; pp. 186–224.
21. SGSS-EMR. Geological, Seismic and Soil Survey of the Emilia-Region: Cartografia. 2019. Available online: https://applicazioni.regione.emilia-romagna.it/cartografia_sgss/user/viewer.jsp (accessed on 31 May 2021).
22. Cervi, F.; Marcaccio, M.; Petronici, F.; Borgatti, L. Hydrogeological characterization of peculiar Apenninic springs. *Proc. Int. Assoc. Hydrol. Sci.* **2014**, *364*, 333–338. [CrossRef]
23. ARPAE-EMR. Regional Agency for Environmental Protection in Emilia-Romagna Region: Annali Idrologici. 2019. Available online: https://www.arpae.it/sim/ (accessed on 31 May 2021).
24. Cervi, F.; Blöschl, G.; Corsini, A.; Borgatti, L.; Montanari, A. Perennial springs provide information to predict low flows in mountain basins. *Hydrol. Sci. J.* **2017**, *62*, 2469–2481. [CrossRef]
25. Municipality of Scandiano. Seismic Analyses and geological Feasibility Study.Geological, Hydrogeological and Seismic Framework in Support of the Municipal Structural Plan. Available online: https://www.comune.scandiano.re.it/piano-strutturale-comunale/quadro-conoscitivo-geologico/ (accessed on 31 May 2021).
26. ATERSIR-RE. Integrated Water Service Area Plan for the Reggio Emilia Province. 2019. Available online: http://www.atersir.it/servizio-idrico/territorio-provinciale-di-reggio-emilia/piano-dambito (accessed on 31 May 2021).
27. Farina, M.; Marcaccio, M.; Zavatti, A. *Esperienze e Prospettive nel Monitoraggio Delle Acque Sotterranee. Il Contributo Dell'emilia-Romagna*; Quaderni di Tecniche di Protezione Ambientale, Pitagora Editrice: Bologna, Italy, 2014; p. 560.
28. Martinelli, G.; Chahoud, A.; Dadomo, A.; Fava, A. Isotopic features of Emilia-Romagna region (North Italy) groundwaters: Environmental and climatological implications. *J. Hydrol.* **2014**, *519*, 1928–1938. [CrossRef]
29. Leibundgut, C.; Maloszewski, P.; Külls, C. *Tracers in Hydrology*; John Wiley & Sons: Hoboken, NJ, USA, 2011.
30. Tazioli, A. Experimental methods for river discharge measurements: Comparison among tracers and current meter. *Hydrol. Sci. J.* **2011**, *56*, 1314–1324. [CrossRef]
31. Vizzi, L. Studio idrogeologico delle sorgenti Mulino delle Vene (Val Tresinaro). Master's Thesis, University of Modena and Reggio Emilia, Modena, Italy, 2013; 101p. Available online: https://morethesis.unimore.it/ETD-db/ETD-search/search (accessed on 31 May 2021).
32. Guizerix, J.; Florkowski, T. Streamflow measurements. In *Guidebook on Nuclear Techniques in Hydrology, 65–80*; IAEA, International Atomic Energy Agency: Vienna, Austria, 1983; ISBN 92-0-145083.
33. Taylor, J.R. *An Introduction to Error Analysis: The Study of Uncertainties in Physical Measurements*, 2nd ed.; University Science Books: Sausalito, CA, USA, 1997.
34. Davis, J.C. *Statistics and Data Analysis in Geology*; John Wiley & Sons: New York, NY, USA, 2001.
35. Doornik, J.A.; Hansen, H. An omnibus test for univariate and multivariate normality. *Oxf. Bull. Econ. Stat.* **2008**, *70*, 927–939. [CrossRef]
36. Breusch, T.S.; Pagan, A.R. A Simple Test for Heteroscedasticity and Random Coefficient Variation. *Econometrica* **1979**, *47*, 1287. [CrossRef]
37. Durbin, J.; Watson, G.S. Testing For Serial Correlation in Least Squares Regression: I. *Biometrika* **1950**, *37*, 409–428.
38. Day, T.J. On the precision of salt dilution gauging. *J. Hydrol.* **1976**, *31*, 293–306. [CrossRef]

39. Day, T.J. Observed mixing lengths in mountain streams. *J. Hydrol.* **1977**, *36*, 125–136. [CrossRef]
40. Poulain, A.; Marc, V.; Gillon, M.; Mayer, A.; Cognard-Plancq, A.L.; Simler, R.; Babic, M.; Leblanc, M. Enhanced pumping test using physicochemical tracers to determine surface-water/groundwater interactions in an alluvial island aquifer, river Rhône, France. *Hydrogeol. J.* **2021**, *29*, 1569–1585. [CrossRef]